Pergamon

Int. J. Heat Mass Transfer. Vol. 38, No. 3, pp. 557–562, 1995

0017–9310/95 $9.50+0.00

0017–9310(94)00172–3

Simple theoretical approach to direct-contact condensation on subcooled liquid film

J. MIKIELEWICZ
Institute of Fluid Flow Machines, Polish Academy of Sciences, ul. Gen. J. Fiszera 14, 80-952 Gdańsk, Poland

and

A. M. A. RAGEB
Mechanical Engineering Department, University of Basrah, Basrah, Iraq

(*Received* 2 *June* 1993)

Abstract—This work presents an approximate theoretical solution of the direct-contact condensation problem. The analysis is based on a simplified energy equation, in which both velocity and temperature gradients in the direction of the liquid flow are taken from the average energy balance. The theoretical results obtained were compared with experimental results from other authors. Satisfactory agreement was obtained.

1. INTRODUCTION

Film condensation phenomena have been studied by many investigators, beginning with Nusselt [1], who investigated the laminar film flow condensation under certain specified assumptions. Later on this model was modified by adding the contribution of the sensible heat term to a heat transfer coefficient. Rohsenow [2] has included the effect of cross flow on heat transfer (convection in flow direction) within the film. However, direct-contact condensation, where steam flow is being condensed onto a thick layer of cold liquid, with negligible heat transfer to the solid boundary, has hardly been studied. The condensation heat transfer in direct-contact mode may be encountered in a variety of industrial applications, such as reflux condenser and tubular contractor. In recent years, the modelling of direct-contact condensation heat transfer has been of major importance in connection with the analysis of nuclear reactor safety systems [3–5]. In the case of loss of coolant in a pressurized water reactor, the emergency cooling water is injected into the pressure vessel to prevent overheating. When the subcooled water is brought into contact with the escaping steam, then direct-contact condensation occurs.

The complexity of the thermo-hydrodynamic coupling of the liquid and vapour phases has resulted in a large number of correlations, including some empirical ones and theoretical works.

The main objective of the present work is to establish a simplified, approximated theoretical solution for direct-contact condensation. This was done by developing a model based on the mass, momentum and energy conservation equations, in addition to the overall heat balance equation. The solution resulted in a more detailed description of flow behaviour, and heat and mass transfer.

2. ANALYTICAL APPROACH

Consider steady, laminar flow of a liquid layer on an adiabatic solid surface, with inlet mass flow rate $\dot{m}_o$ and subcooled inlet temperature T_o. Steam with saturation temperature T_s flows concurrently with the liquid layer and condenses on the liquid free surface (Fig. 1). Both the gravity and the shear stress are the means of driving the liquid layer. Any instabilities or waves which may be present due to steam upflow are neglected. Using these assumptions, the simplified heat balance for a control volume, therefore, is

$$\dot{m}c_p\,\mathrm{d}T_f = h_{fg}\,\mathrm{d}\dot{m} = qb\,\mathrm{d}x = h_x b(T_s - T_f)\,\mathrm{d}x \quad (1)$$

or

$$\dot{m}c_p\frac{\mathrm{d}T_f}{\mathrm{d}x} = h_{fg}\frac{\mathrm{d}\dot{m}}{\mathrm{d}x} \quad h_x = \frac{h_{fg}}{b(T_s - T_f)}\frac{\mathrm{d}\dot{m}}{\mathrm{d}x}. \quad (2)$$

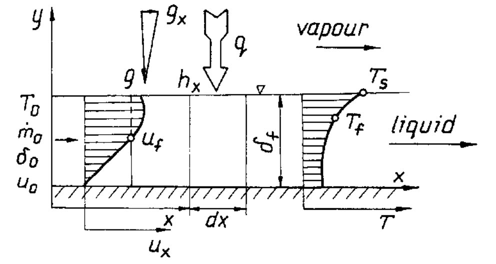

Fig. 1. Direct-contact condensation model.

NOMENCLATURE

- A area [m^2]
- b width of the liquid film [m]
- c_p specific heat at constant pressure [J kg^{-1}K^{-1}]
- G gravity parameter, $g\delta_o^2/\nu u_o$
- g acceleration due to gravity [m s^{-2}]
- h heat transfer coefficient [W m^{-2} K^{-1}]
- h_{fg} latent heat of evaporation [J kg^{-1}]
- k thermal conductivity [W m^{-1} K^{-1}]
- M function defined by equation (35b)
- $\dot{m}$ mass flow rate [kg s^{-1}]
- $\overline{Nu}$ average Nusselt number, $\bar{h}\delta_o/k$
- Pe Peclet number, $u_o\delta_o/\alpha$
- q heat flux [W m^{-2}]
- S subcooling number, $c_p(T_s-T_f)/h_{fg}$
- T temperature, shear stress parameter, $\tau_s\delta_o/\rho\nu u_o$
- u velocity in direction of flow [m s^{-1}]
- x coordinate in direction of flow [m]
- y coordinate normal to the flow [m].

Greek symbols
- α thermal diffusivity [m^2 s^{-1}]
- δ liquid layer thickness [m]
- μ dynamic viscosity [kg m^{-1} s^{-1}]
- ν kinematic viscosity [m^2 s^{-1}]
- ρ density [kg m^{-3}]
- τ shear stress [kg m^{-1} s^{-2}].

Subscripts
- f average over cross-section of flow
- o at the inlet
- s saturated
- x local.

Superscripts
- $+$ nondimensional
- $-$ average over the axial length.

Other terms in the heat balance equation were neglected, since

$$h_{fg} \gg c_p(T_s-T_f).$$

Before proceeding further, it is convenient to bring this equation into dimensionless form. With

$$x^+ = \frac{x}{\delta_o} \tag{3a}$$

$$y^+ = \frac{y}{\delta_o} \tag{3b}$$

$$\dot{m}^+ = \frac{\dot{m}}{\dot{m}_o} \tag{3c}$$

$$T_f^+ = \frac{T_s-T_f}{T_s-T_o} \tag{3d}$$

equation (2) becomes

$$-\frac{dT_f^+}{dx^+} = \frac{1}{S\dot{m}^+}\frac{d\dot{m}^+}{dx^+} \tag{4a}$$

where

$$S = \frac{c_p(T_s-T_o)}{h_{fg}}. \tag{4b}$$

Equation (4a) cannot be integrated without evaluation of the $\dot{m}$; therefore, from the momentum and continuity equations the velocity distribution may be obtained and can be written in the following form:

$$u^+ = \frac{u}{u_o} = -\frac{1}{2}\frac{g\delta_o^2}{\nu u_o}y^{+2} + \left(\frac{\tau_s\delta_o}{\rho\nu u_o} + \frac{g\delta_o^2\delta^+}{\nu u_o}\right)y^+ \tag{5}$$

or

$$u^+ = -\tfrac{1}{2}Gy^{+2} + (T+G\delta^+)y^+ \tag{6a}$$

where

$$T = \frac{\tau_s\delta_o}{\rho\nu u_o} \tag{6b}$$

and

$$G = \frac{g\delta_o^2}{\nu u_o}. \tag{6c}$$

The average velocity over the cross-section of the flow at any distance from the inlet is given by

$$u_f^+ = \tfrac{1}{3}G\delta^{+2} + \tfrac{1}{2}T\delta^+ \tag{7}$$

and the dimensionless mass flow rate is

$$\dot{m}^+ = \tfrac{1}{3}G\delta^{+3} + \tfrac{1}{2}T\delta^+. \tag{8}$$

Therefore substitution of equation (8) and

$$\frac{d\dot{m}^+}{dx^+} = (G\delta^{+2}+T\delta^+)\frac{d\delta^+}{dx^+} \tag{9}$$

into equation (4a) results in

$$\frac{dT_f^+}{dx^+} = -\frac{1}{S}\frac{G\delta^{+2}+T\delta^+}{\frac{1}{3}G\delta^{+3}+\frac{1}{2}T\delta^{+2}}\frac{d\delta^+}{dx^+}. \tag{10}$$

Integrating equation (10), subjected to the boundary conditions

$$T_f^+ = 1 \quad \text{at} \quad \delta^+ = 1 \tag{11}$$

gives

$$T_f^+ = \frac{1}{S}\ln\left|\frac{\frac{1}{3}G+\frac{1}{2}T}{\frac{1}{3}G\delta^{+3}+\frac{1}{2}T\delta^{+2}}\right| + 1. \tag{12}$$

It thus appears that T_f^+ is undetermined from equation (12), since there is no other relation to determine the δ^+. The following approach proposed to estimate δ^+ is considered to be the main point characterizing this work. This was done through estimation of a new solution for T_f^+ using a specific form of the energy equation instead of the heat balance equation used previously. The appropriate energy equation has the following form:

$$\frac{\partial^2 T}{\partial y^2} = \frac{u_f}{\alpha}\frac{dT_f}{dx}. \tag{13}$$

It should be noticed here that the right-hand side of the above equation is a function of x only. Such an assumption may lead to error; however, this becomes ineffective for a thin liquid layer or well mixed flow.

Introducing the dimensionless variables into equation (13), it becomes

$$\frac{\partial^2 T^+}{\partial y^{+2}} = Pe\, u_f^+ \frac{dT_f^+}{dx^+} \tag{14a}$$

where

$$T^+ = \frac{T_s - T}{T_s - T_o} \tag{14b}$$

$$u_f^+ = \frac{u_f}{u_o} \tag{14c}$$

and

$$Pe = \frac{u_o \delta_o}{\alpha} \tag{14d}$$

with boundary conditions

$$\frac{\partial T^+}{\partial y^+} = 0 \quad \text{at} \quad y^+ = 0 \tag{15a}$$

$$T^+ = 0 \quad \text{at} \quad y^+ = \delta^+. \tag{15b}$$

Substitution of u_f^+ and dT_f^+/dx^+ from equations (7) and (10), respectively, into equation (14a) gives

$$\frac{\partial^2 T^+}{\partial y^{+2}} = -\frac{Pe}{S}(G\delta^+ + T)\frac{d\delta^+}{dx^+}. \tag{16}$$

Integrating equation (16) and fulfilling the boundary conditions (15a), (15b) yields

$$T^+ = \frac{1}{2}\frac{Pe}{S}(G\delta^+ + T)(\delta^{+2} - y^{+2})\frac{d\delta^+}{dx^+}. \tag{17}$$

In order to find the temperature T_f^+ defined by equation (3d), the definition of the bulk temperature may be used:

$$T_f^+ = \frac{\int_0^{\delta^+} u^+ T^+ \, dy^+}{\int_0^{\delta^+} u^+ \, dy^+}. \tag{18}$$

Substitution of equations (6a), (17) into equation (18) and integrating results in

$$T_f^+ = \frac{1}{2}\frac{Pe}{S}(G\delta^+ + T)\frac{\frac{11}{60}G\delta^{+5} + \frac{1}{4}T\delta^+}{\frac{1}{3}G\delta^{+3} + \frac{1}{2}T\delta^{+2}}\frac{d\delta^+}{dx^+}. \tag{19}$$

Comparison of equation (12) with equation (19) enables us to find the value of $d\delta^+/dx^+$, which may be written in the form

$$\frac{d\delta^+}{dx^+} = -\frac{\dfrac{1}{S}\ln\left|\dfrac{\frac{1}{3}G + \frac{1}{2}T}{\frac{1}{3}G\delta^{+3} + \frac{1}{2}T\delta^{+2}}\right|}{\dfrac{1}{2}\dfrac{Pe}{S}(G\delta^+ + 1)\dfrac{\frac{11}{60}G\delta^{+5} + \frac{1}{4}T\delta^{+4}}{\frac{1}{3}G\delta^{+3} + \frac{1}{2}T\delta^{+2}}}. \tag{20}$$

Determination of liquid layer thickness

The thickness of the liquid layer can be estimated for the following cases.

Case 1. $T = 0$, the liquid layer is driven by gravitational force only; equation (20) is reduced to

$$dx^+ = \frac{11}{40}\frac{Pe \cdot G}{S}\frac{\delta^{+3}\, d\delta^+}{-3 \cdot \dfrac{1}{S}\ln\delta^+ + 1}. \tag{21}$$

Since the expected value of δ^+ is almost 1, then it is possible to write

$$\ln\delta^+ = \delta^+ - 1. \tag{22}$$

After introducing equation (22) into equation (21) and some rearrangement, it is possible to integrate equation (21) analytically and eventually get

$$\frac{40}{11}\frac{x^+}{Pe \cdot G} = -\frac{1}{9}(\delta^{+3} - 1) - \frac{1}{18}S\left(3 \cdot \frac{1}{S} + 1\right)(\delta^{+2} - 1)$$

$$-\frac{1}{27}S^2\left(3 \cdot \frac{1}{S} + 1\right)^2(\delta^+ - 1) - \frac{1}{81}S\left(3 \cdot \frac{1}{S} + 1\right)^3$$

$$\times \ln\left|-3 \cdot \frac{\delta^+}{S} + 3 \cdot \frac{1}{S} + 1\right|. \tag{23}$$

The above equation can be used to calculate the thickness δ^+ for any value of x^+.

Case 2. $G = 0$, the liquid layer is driven by shear stress only; equation (20) is reduced to

$$dx^+ = \frac{1}{4}\frac{Pe \cdot T}{S}\frac{\delta^{+2}\, d\delta^+}{-2 \cdot \dfrac{1}{S}\ln\delta^+ + 1}. \tag{24}$$

Using the approximation given by equation (22) in equation (24), after rearrangement it is possible to integrate the equation analytically to obtain eventually

$$16\frac{x^+}{Pe \cdot T} = -(\delta^{+2} - 1) - S\left(2 \cdot \frac{1}{S} + 1\right)(\delta^+ - 1)$$

$$-\frac{1}{2}S^2\left(2 \cdot \frac{1}{S} + 1\right)^2 \ln\left|-2 \cdot \frac{\delta^+}{S} + 2 \cdot \frac{1}{S} + 1\right|. \tag{25}$$

From this equation the value of δ^+ could be calculated for any x^+.

Case 3. $T \neq 0$, $G \neq 0$, both gravity force and shear stress are acting; the value of δ^+ could be calculated numerically using equation (20).

Heat transfer coefficient

The local heat transfer coefficient may be obtained from heat balance (1):

$$h_x = \frac{h_{fg}}{b(T_s - T_f)} \frac{d\dot{m}}{dx}. \tag{26}$$

The average heat transfer coefficient may be estimated, based on the heat balance, to get

$$\bar{h} = \frac{h_{fg}}{bx(T_s - \bar{T}_f)} \int_0^x d\dot{m}. \tag{27}$$

Using equations (26) and (27), both h_x and $\bar{h}$ for $b = 1$ m can be estimated for the following cases.

Case 1. $T = 0$, the liquid layer is driven by gravity force only. Substitution of equations (9) and (12) for $T = 0$ in equation (26) gives

$$h_x = \frac{40}{11} \frac{k}{\delta}. \tag{28}$$

The average heat transfer coefficient is evaluated through obtaining an expression for $(T_s - \bar{T}_f)$ by integrating equation (12) and averaging it. The length in flow direction with respect to the final result may be written in the form

$$\frac{(T_s - \bar{T}_f)}{(T_s - T_o)} = \frac{11}{60} \frac{Pe \cdot G}{S \cdot x^+} (\delta^{+4} - 1). \tag{29}$$

Then substituting equations (9) and (29) into equation (27) and integrating it gives the final result in Nusselt number form, as

$$\overline{Nu} = \frac{160}{33} \left(\frac{\delta^{+3} - 1}{\delta^{+4} - 1} \right). \tag{30}$$

Case 2. $G = 0$, the liquid layer is driven by shear stress only. Substitution of equations (9) and (12) for $G = 0$ in equation (26) gives

$$h_x = 4 \frac{k}{\delta}. \tag{31}$$

In a manner similar to that of case 1, the average Nusselt was obtained first through finding $(T_s - \bar{T}_f)$, which is given by

$$\frac{T_s - \bar{T}_f}{T_s - T_o} = \frac{1}{12} \frac{Pe \cdot T}{S \cdot x^+} (\delta^{+4} - 1). \tag{32}$$

Then the average Nusselt number is given by

$$\overline{Nu} = 6 \left(\frac{\delta^{+2} - 1}{\delta^{+3} - 1} \right). \tag{33}$$

Case 3. $G \neq 0$, $T \neq 0$, both gravity force and shear stress are acting. Similarly, the local heat transfer coefficient could be estimated to get

$$h_x = 4 \frac{k}{\delta} \left(\frac{\frac{1}{3} G \delta^+ + \frac{1}{2} T}{\frac{11}{30} G \delta^+ + \frac{1}{2} T} \right) \tag{34}$$

and the average heat transfer coefficient in the form of average Nusselt number is obtained:

$$\overline{Nu} = \frac{2[\frac{1}{3} G(\delta^{+3} - 1) \frac{1}{2} T(\delta^{+2} - 1)]}{M} \tag{35a}$$

where

$$M = \frac{11}{80} G(\delta^{+4} - 1) + \frac{19}{120} T(\delta^{+3} - 1) + \frac{3}{160} \frac{T^2}{G} (\delta^{+2} - 1) - \frac{9}{160} \frac{T^3}{G^2} (\delta^+ - 1) + \frac{27}{320} \frac{T^4}{G^3} \ln \left| \frac{2\delta^+ + 3T}{2G + 3T} \right|. \tag{35b}$$

3. RESULTS AND DISCUSSION

The values of gravity and shear stress parameters (G and T) are needed in order to perform calculations. Those parameters are interrelated through equation (8), and for the inlet conditions this equation becomes

$$1 = \tfrac{1}{3} G + \tfrac{1}{2} T. \tag{36}$$

Calculations of the liquid layer thickness and the average Nusselt number were carried out for a number of selected values of the gravity and shear stress parameters which were determined from equation (36). For a better understanding of the influence of the related parameters on the condensation process, the results are plotted against the axial position, as shown in Figs. 2–7. The graph of dimensionless thickness δ^+ against the axial distance is shown in Figs. 2–4. The observed increase in δ^+ with increment of x^+ is due to the continuous condensation at the liquid–vapour interface. Figure 2 is drawn for various values of Peclet number, while the other control parameters (G, T and S) are kept constant. The effect of variation of Peclet number on δ^+ shows a significant decrement in δ^+ with increment of Peclet number. This is due to the more rapid growth of initial thickness than the local thickness of the liquid layer. The influence of changes

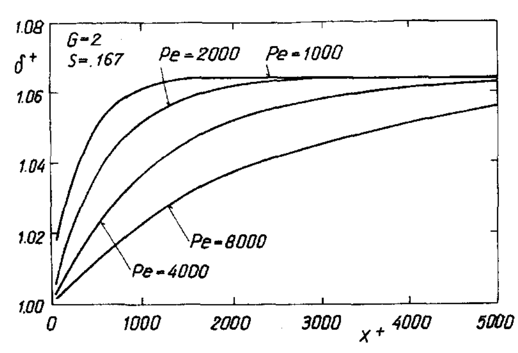

Fig. 2. Dimensionless thickness vs the axial distance for different values of Peclet number.

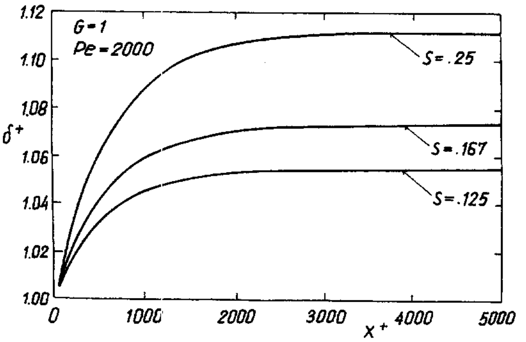

Fig. 3. Dimensionless thickness vs the axial distance for different values of subcooling number.

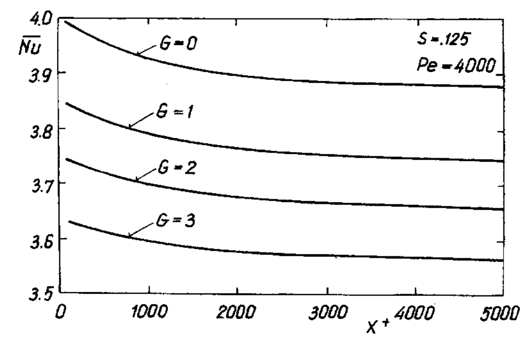

Fig. 7. Average Nusselt number vs the axial distance for different values of gravity parameter.

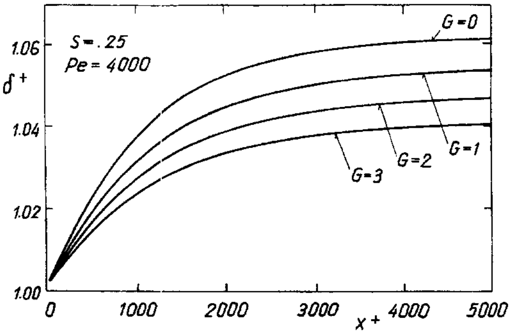

Fig. 4. Dimensionless thickness vs the axial distance for different values of gravity parameter.

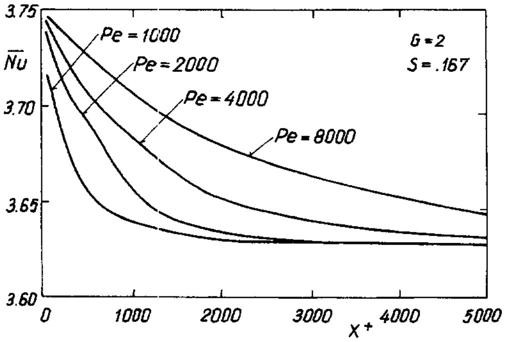

Fig. 5. Average Nusselt number vs the axial distance for different values of Peclet number.

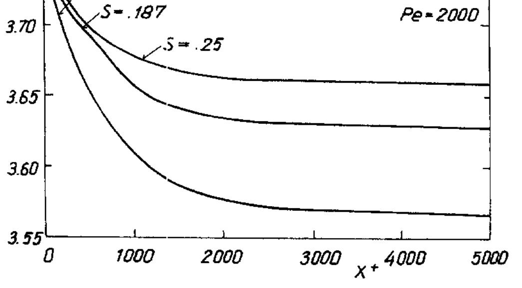

Fig. 6. Average Nusselt number vs the axial distance for different values of subcooling number.

in the subcooling number S on the liquid layer thickness is illustrated in Fig. 3. This figure indicates that the decrease in S is accompanied by a decrease in δ^+. This is due to the corresponding decrease in the heat transfered through the free liquid surface. Other parameters which may have an effect on δ^+ are related to the means of driving the liquid layer. These are the gravity and shear stress parameters. The behaviour of δ^+ for different values of G and T [obtained according to equation (36)] is shown in Fig. 4. The maximum values of δ^+ are corresponding to $G = 0$ or $T = 2$, while the minimum values of δ^+ occur at $G = 3$ or $T = 0$. This may be attributed to both the changes in the thickness of the cold liquid layer without condensation, and the enhancement of heat transfer at the liquid–vapour interface during condensation. Comparing the results of Figs. 2–4, it can be noticed that the variation of the subcooling number S is influencing δ^+ more than the Peclet number or the gravity and shear stress parameters.

Average Nusselt number was calculated and drawn in Figs. 5–7 against the axial position. The general trend visible in those figures is the decrement of Nusselt number along the axial position, while the heat transfer coefficient decreases. This is due to the increment of the liquid layer thickness. From Figs. 5 and 6 it appears that the variation of Nusselt number is much less pronounced in comparison with the variation of Peclet number or the subcooling number. This can be explained through the relation between the thickness of the flowing liquid layer and the heat transfer coefficient. Increasing the subcooling number or Peclet number will lead to a thick liquid layer, and in turn diminishes the heat transfer coefficient [equations (28), (31), (34)]. Therefore, both mentioned parameters (Pe and S) may lead to a small change in Nusselt number. Figure 7 shows $\overline{Nu}$ as a function of x^+ for various values of gravity and shear stress parameters. While the other parameters are kept constant, the average Nusselt number is inversely proportional to the gravity parameter and directly proportional to the shear stress parameter.

To prove the validity of the present approach, the results obtained were compared with data corresponding to the countercurrent flow on a nearly

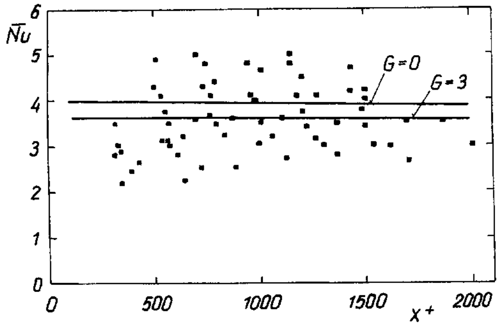

Fig. 8. Comparison between the present theory and the experimental data of Bankoff and Lee [6].

vertical channel (87° to the horizontal), obtained by Bankoff and Lee [6]. Theoretical results calculated from equations (30) and (33) indicate two extreme cases of flow conditions; gravity and shear drive. The data taken from Bankoff and Lee [6], and the results of the present theory, are presented in Fig. 8. The scattered points visible in this figure correspond either to the relatively high Rynolds number, or to the thick liquid layer. This discrepancy can be explained by the simplifying restrictions imposed on the model. The assumption of the constant velocity and temperature gradients used in the energy equation may have a negligible effect on the solution for the thin liquid layer. For the thick layer, however, the effect is more pronounced, and may lead to some appreciable error. The comparison is based on the available data and, unfortunately, these do not satisfy all the requirements of the model. This may be considered as another reason for the discrepancy apparent in Fig. 8. In spite of those conditions, the agreement between the present theory and the experimental results has justified the validity of the model.

4. CONCLUSIONS

The main points which can be drawn from the above analysis and discussion are:

(1) an adequate solution for the direct-contact condensation was obtained;

(2) the solution considers only a few parameters controlling the process—the Peclet number, the subcooling number, gravity and shear stress parameters;

(3) the major effect on the liquid layer thickness is attributed to the subcooling number, while the effect of the other parameters is less significant;

(4) only about 10% of variation in the average Nusselt number was observed for the two extreme cases—the gravity or shear stress driven film cases.

REFERENCES

1. W. Nusselt, Die Oberflachenkondensation des Wasserdampfes, *Z. Vereines Deutscher Ingenieure* **60,** 541–546, 569–576 (1916).
2. W. M. Rohsenow, Heat transfer and temperature distribution in laminar film condensation, ASME Paper No. 54-A-144 (1954).
3. S. G. Bankoff and H. J. Kim, Local condensation rates in a nearly horizontal stratified countercurrent flow of steam and cold water, *AIChE Symp. Ser.* **79,** 209–223 (1983).
4. A. Segev and R. P. Collier, A mechanistic model for countercurrent steam–water flow, *Trans. ASME J. Heat Transfer* **102,** 688–693, (1980).
5. S. G. Bankoff, Some condensation studies pertinent to LWR safety, *Int. J. Multiphase Flow* **6,** 51–67 (1980).
6. S. G. Bankoff and S. C. Lee, Condensation in stratified flow, Dataset No. 16. In *Multiphase Science and Technology*, Vol. 3, pp. 398–422. Hemisphere, New York (1987).